

600W DC to DC LLC Design Using GaN FETs

600W DC to DC LLC Design Using GaN FETs

1. Introduction

Many people still debate whether global warming is real, and, if so, whether human behavior impacts it. Inarguably, 2018 is the fourth hottest year in history; July is California’s hottest month on record [1]; and CO₂ emissions are known to affect climate change.

The Information and Communication Technology (ICT) sector generates over 2% of the global CO₂ emissions. Data centers are the fastest growing segment within ICT and account 1.4% of global electricity consumption. That percentage is expected to increase at faster rates due partly to the rapidly growing use of cloud computing and Internet services [2].

High efficiency AC to DC and DC to DC power supplies using GaN can reduce energy loss by 50%, which would then reduce CO₂ emissions. Soft-switching topologies capable of operating at high frequencies while reducing switching losses are optimal for such power supplies—with the more commonly preferred choice being the LLC resonant topology as it offers the following advantages:

- Zero-voltage Switching (ZVS), which produces high efficiency and enables the transformer size to shrink due to high frequency use.
- Limited dv/dt and di/dt, which reduces ringing, spikes, and radiated EMI problems.

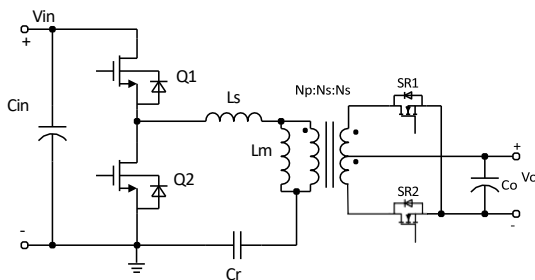


Figure 1. Schematic of half bridge LLC resonant converter

2. LLC Converter Description

Figure 1 shows the half bridge LLC topology including the full wave synchronous rectified circuit, where the Ls is the series resonant inductor, Lm is the magnetizing inductor, and Cr is the resonant capacitor. Q1 and Q2 are typically operating in 50% duty cycle square waveform with variable switching frequency. The series resonant converter (SRC) then behaves as if it has a resonant frequency:

$$f_0 = \frac{1}{2\pi\sqrt{L_s C_r}} \quad (1)$$

To achieve ZVS at turn on, the current *i_L* should lag *V_{sw}*, i.e. the output impedance seen from the switching node should be inductive, as shown in Figure 2. Therefore, the switching frequency *f_{sw}* must be higher than the resonant frequency *f_o*. However, the drawbacks for SRC operating in *f_{sw}* > *f_o* are non-zero-current-switching (ZCS) on the secondary side SR-MOSFETs and <1 voltage gain. By introducing a paralleled inductor with transformer, the inductive current (*i_{Lm}*) is obtained when *f_{sw}* < *f_o*, and will not translate into the secondary side so ZCS can be achieved in the same time.

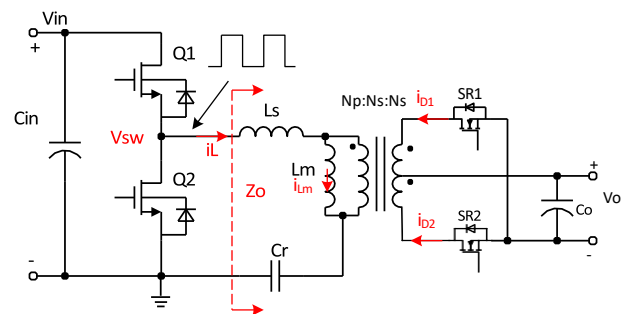


Figure 2. To achieve ZVS on primary side and ZCS on secondary side, *f_{sw}* < *f_o* and Zo should be inductive. So, Lm is introduced.

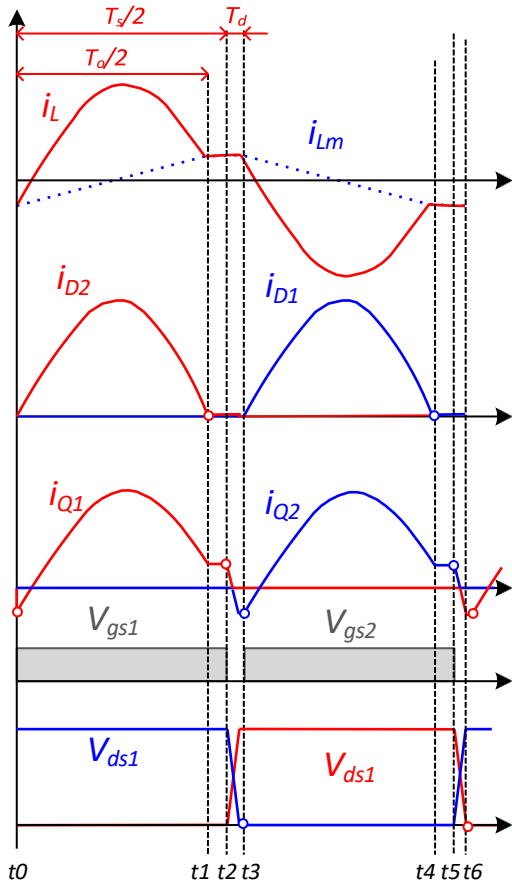


Figure 3. Typical waveform of the half bridge LLC converter at $f_{sw} < f_o$

Figure 3 shows the typical waveforms of a half bridge LLC converter at $f_{sw} < f_o$. At t_0 , the current i_L is negative, so Q1 is freewheeling, hence achieving soft-switching turning on. The voltage applies on the resonant tank and resonant current changes with the frequency f_o . On the other hand, the magnetizing inductor is charging. When the resonant current goes back to 0A at t_1 , the secondary side i_{D2} reduces to 0 as well to achieve ZCS. Since $f_{sw} < f_o$, when the Q1 turns off, the magnetizing current flows through the body diode of Q2, so that during the dead time the Coss can be discharged and V_{ds_Q2} reduces to 0 before it turns on. The relation between magnetizing current and dead time will be discussed in the following section. The current i_{D2} resonances to 0 A before Q1 turns off, so zero current turn-off is achieved on the secondary side.

Another resonant frequency is determined by L_p , L_s and C_r :

$$f_{o2} = \frac{1}{2\pi\sqrt{(L_m+L_s)C_r}} \quad (2)$$

When the load is getting heavier, the switching frequency will keep reducing to achieve higher gain, but the switching frequency f_{sw} should be higher than f_{o2} to avoid hard switching turn-on.

In this application note, a 48V/600W LLC converter is designed, and the input/output specifications are as follow:

- Input: 380Vdc nominal (320V-400V)
- Output: 48Vdc at 12.5A
- Switching Frequency: 170kHz to 250 kHz

3. Parameters Design

3.1 Transformer Turns Ratio

For the 48V output, the input voltage varies in a small voltage range $V_{in} \in [320V, 400V]$. Since the LLC converter has the voltage boost function, the turns ratio can be selected according to the maximum input voltage, i.e. For full waveform rectifier, $N_p : N_s = V_{in,max} / (2 \cdot V_o) = 25 : 6$.

3.2 LLC Converter Gain Calculation (integrated transformer)

As discussed in section 2, the LLC converter operates in soft-switching condition when switching frequency $f_{o2} < f_{sw} < f_o$. The LLC converter also provides boost function in this area. Based on the fundamental harmonics analysis method (FHA), the AC equivalent circuit referred to the primary side can be drawn in Figure 4.

$$M_V = \sqrt{\frac{L_p}{L_p - L_s}} = \sqrt{\frac{L_n}{L_n - 1}} \quad (3)$$

$$R_{ac} = \frac{M_V 8n^2}{\pi^2} R_L \quad (4)$$

$$G = \frac{V_o^F}{V_{in}^F} = \frac{j\omega L_m / R_{ac}}{j\omega C_r + j\omega L_r + j\omega L_m / R_{ac}} \quad (5)$$

$$|G| = \frac{M_V}{\sqrt{(f_n - \frac{1}{f_n})^2 (1 - \frac{1}{L_n})^2 Q^2 + (1 + \frac{1}{L_n} \frac{1}{f_n^2 L_n})^2}} \quad (6)$$

Where $L_n = L_p / L_s$, $f_n = f_{sw} / f_o$, $Q = \sqrt{L_s} / R_{ac}$.

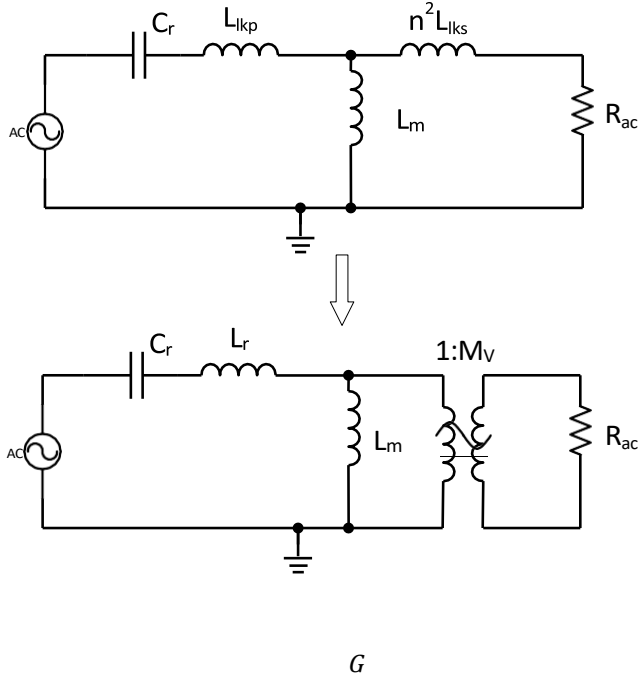


Figure 4. AC Equivalent Circuit referred to primary side

From (6), the gain varies with the frequency and the load. As drawn in Fig. 5, the gain curve changes with the switching frequency. At resonant frequency, the gain is equal to $\sqrt{L_n / (L_n - 1)}$, and the gain increases as the switching frequency decreases. However, when the load increases, the peak voltage gain reduces. In the green area, the converter is operating in ZVS at primary side and ZCS at secondary side, so the efficiency keeps high. When the load increases, the peak voltage gain decreases, and the converter may enter the red area where its primary side switches lose ZVS and results in hard-switching. For a proper designed converter, the red area should be avoided. To maintain the soft-switching condition and to meet the gain requirement at the minimum input voltage, the L_n and Quality Factor (Q) should be analyzed.

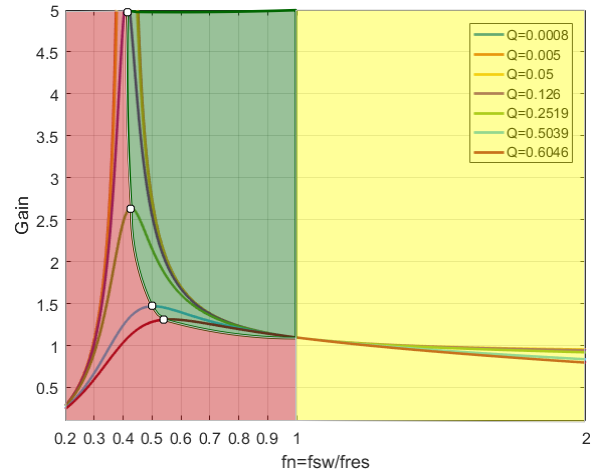


Figure 5. Gain curve versus frequency ($L_n=5$).
 Red Area: capacitive operation range, ZCS
 Green Area: inductive operation range, ZVS
 Yellow Area: inductive operation range, ZVS

For the minimum input voltage of 320V, the required gain is:

$$G_{max} = \frac{2V_o}{V_{in_min}} \cdot \frac{N_{pri}}{N_{sec}} = 1.25 \quad (7)$$

Considering a 20% margin for overcurrent capability, peak gain should be >1.5 .

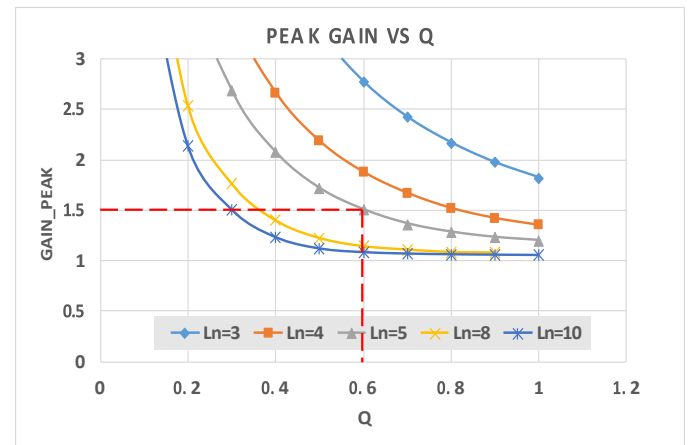


Figure 6. Peak Gain versus Q for different L_n [?]

Figure 6 plots the peak gain versus Q at full load in different L_n values. By rewriting the L_s and C_r as:

$$\begin{cases} C_r = \frac{1}{2\pi R_{ac} f_0 Q} \\ L_s = \frac{R_{ac} L_0 Q}{2\pi f_0} \\ L_p = L_n L_s \end{cases} \quad (8)$$

The resulting resonant tank parameters are:

$$C_r = 24.4nF, L_s = 26\mu H, L_p = 130\mu H$$

The voltage gain with different load can be plotted in Figure 7. The switching frequency will change from to at full load with the input voltage range [320V, 400V].

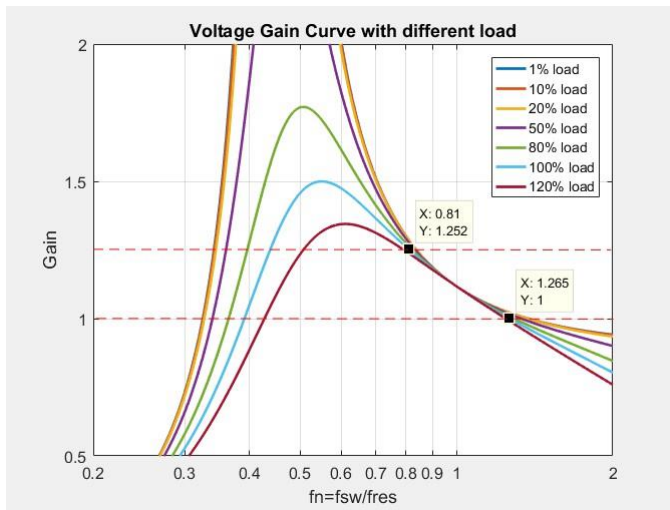


Figure 7. Voltage Gain versus frequency with different load

3.3 LLC voltage gain calculation (separated resonant inductor)

The transformer with integrated leakage inductance can save the external resonant inductor, hence reducing its size. However, the leakage inductance should not be considered just as a “lumped” leakage inductance seen from the primary side, but as primary and secondary leakage inductances (Figure 4) that should be considered separately in the LLC converter. The non-ideal coupling makes the gain curve not match the curve calculated using the FHA method [3], and the leakage inductance on the secondary side will result in voltage rising on the SR-MOSFET especially for high

current, low voltage applications. As a result, higher voltage rating MOSFETs must be chosen.

For the transformer with minimum leakage inductance, the real turns ratio is close to $N_p : N_s$. At resonant frequency, the LLC voltage gain is 1.05 (considering internal $L_p : L_s = 10:1$).

The gain equation in (6) is then modified:

$$|G| = \frac{1.05}{\sqrt{(f_n - \frac{1}{f_n})^2 (1 - \frac{1}{L_n})^2 Q^2 + (1 + \frac{1}{L_n} - \frac{1}{f_n L_n})^2}} \quad (9)$$

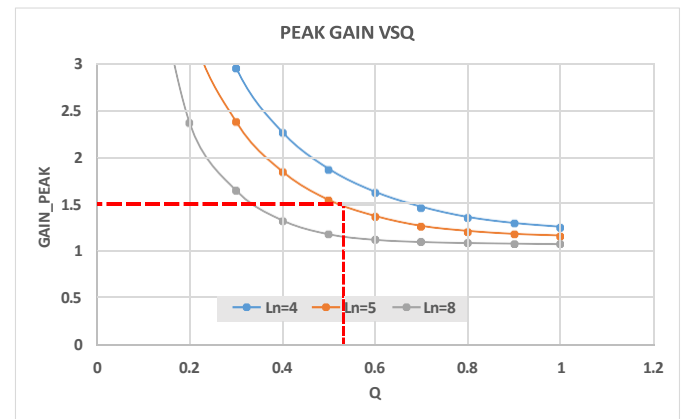


Figure 8. Peak Gain versus Q for different L_n for separated leakage inductance

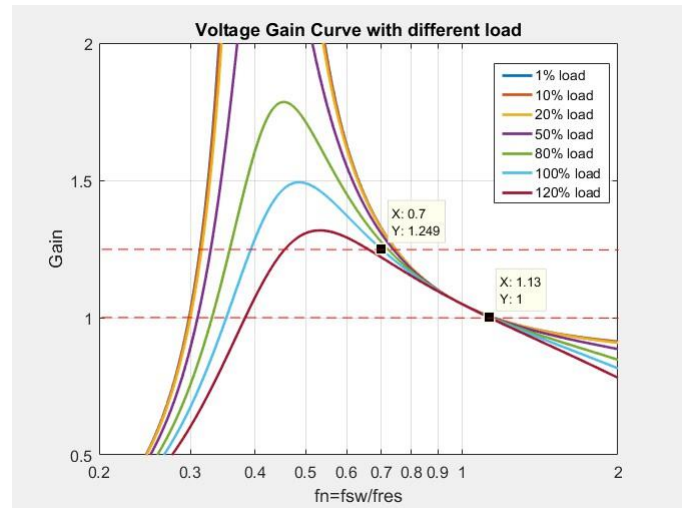


Figure 9. Voltage Gain versus frequency with different load for separated resonant inductor

Using the same method, the peak gain for different L_n and Q is plotted in Figure 8. The resonant tank parameters are then recalculated:

$$C_r = 21nF, L_s = 30\mu H, L_p = 104\mu H$$

The voltage gain shown in Figure 9 notes that the switching frequency range varies between $[0.7, 1.13] \cdot f_o$ according to the different input voltage.

3.4 Dead time calculation

For a 600W LLC converter, the 180mΩ TPH3206PS[4] GaN FETs are selected. During the dead time between high side and low side devices, the turn-off current should be able to discharge the output and stray capacitor, and the dead time should meet:

$$I_{m(on)} \cdot T_d \geq V_{in}(2C_{o(tr)} + C_{stray}) \quad (10)$$

Where $I_{m(on)} = \frac{V_{in} \cdot T_o}{2L_m}$, the dead time can be calculated:

$$T_d \geq \frac{8L_m(2C_{o(tr)} + C_{stray})}{T_o} = 105ns \quad (11)$$

The real dead time is set to 150ns. Table I lists the required $I_{m(on)} \cdot T_d$ with different devices. The GaN FETs outperform the best Si-MOSFETs.

Table 1. Required charge for ZVS

Device	$R_{ds(on)}$	$C_{o(tr)}$	$I_{m(on)} \cdot T_d$
TPH3206	180 mΩ	106 pF	85 nC
TPH3208[5]	110 mΩ	133 pF	107 nC
Si-MOS A	180 mΩ	349 pF	279 nC
Si-MOS B	125 mΩ	579 pF	463 nC
Si-MOS C	144 mΩ	402 pF	322 nC

3.5 Transformer and resonant inductor design

A set of PQ3230/3C95 core is selected for the transformer, and the turns ratio is 25:6:6. The AC flux density is:

$$\Delta B = \frac{V_o}{2N_s A_{eff} f_o} \quad (12)$$

The B_m is 0.5ΔB, which is 0.06T, and the core loss can be calculated by the core loss equation provided by the vendor [6]:

$$P_{core} = V_e C_m f^x B^y (C_{t2} T^2 - C_{t1} T + C_t) / 1000 \quad (13)$$

Where $V_e = 12500mm^3$, for 3C95, $C_m = 7.47m$, $x = 1.955$, $y = 3.070$, $C_{t1} = 0.0126$, $C_{t2} = 0.606\mu$. The core loss is 0.473W at 200kHz.

The rms current in transformer windings can be calculated by the equations (14) and (15):

$$I_{pri}(rms) = \sqrt{\frac{1}{2} \left[\left(\frac{\pi I_o T_s}{2N \cdot T_o} \right)^2 + I_{Lm}^2 \right] \frac{T_o}{T_s} + I_{Lm}^2 \left(1 - \frac{T_o}{T_s} \right)} \quad (14)$$

$$I_{sec}(rms) = I_o \sqrt{\frac{\pi^2 T_s}{11 T_o} + \left(\frac{5}{12} - \frac{a}{\pi^2} \right) \left(\frac{N \cdot I_{Lm}}{I_o} \right)^2 \frac{T_o}{T_s}} \quad (15)$$

For a PQ3230 core, the windows area A_w is 53mm², and .35 is chosen as the window's filling factor, so the effective A_w is 19mm². The total current in both the primary and secondary side windings is:

$$I_{tot} = I_{pri,rms} + \frac{2N_s}{N_p} I_{sec} = 8.8A \quad (16)$$

The winding turn's factor and section area can be determined by:

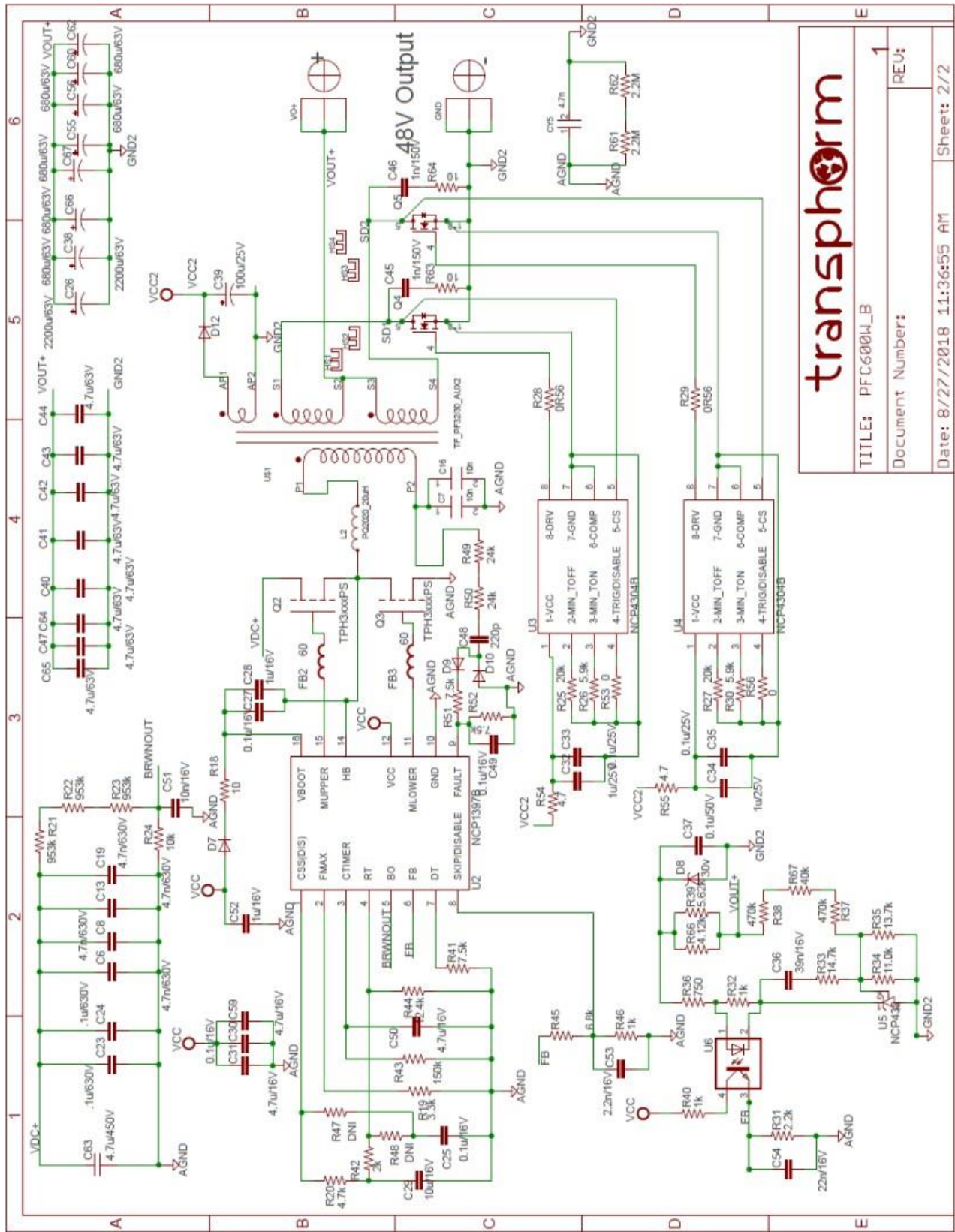
$$w_{pri} = \frac{I_{pri,rms}}{I_{total}}, A_{w,pri} = \frac{w_{pri} \cdot A_{eff}}{N_p}$$

$$w_{sec} = \frac{I_{sec,rms}}{I_{total}}, A_{w,sec} = \frac{w_{sec} \cdot A_{eff}}{N_s}$$

Forty strands of AWG38 litz wire is selected for the primary winding, and 120 strands of AWG 38 litz wire for the secondary. The conduction loss can be calculated by:

$$P_{cond} = I_{pri}^2 \cdot R_{dc,pri} + 2I_{sec}^2 \cdot R_{dc,sec} \quad (17)$$

Where $R_{dc} = \frac{N \rho \cdot MLT}{nw(0.25\pi \cdot d^2)}$, ρ is the copper resistivity coefficient, MLT is the mean length of a turn, nw the strands number of the litz wire, and d is the diameter of each strand of the wire. The total copper loss at full load is 4.45W.



transphorm

TITLE: PFC600W_B	REV: 1
Document Number:	
Date: 8/27/2018 11:36:55 AM	Sheet: 2/2

Figure 10. 600W, LLC design schematic

An additional winding is used to generate the auxiliary power to drive the SR-MOSFET. The magnetizing inductance 110uH is created by gapping the center pole with the leakage inductance minimized to ~3uH. The external 20uH resonant inductor is designed by a PQ2020 core to guarantee no saturation during the start-up high inrush current.

4. Circuit design

The LLC circuit is shown in Page 6. A NCP1397B [7] LLC controller and NCP4304B [8] SR-MOSFET controller are selected for the control realization. An IPB108N15N3 G from Infineon is selected as the SR-MOSFET.

5. Experimental Results

The efficiency is measured under these conditions: the input voltage is from a 600W PFC converter, the input voltage is 385V with 120Hz voltage ripple. The peak efficiency is over 98% from 230W to 420W, as shown in Figure 11. Figure 12 shows the switching node voltage and transformer current waveform on the primary side. The switching frequency is 192kHz and the primary rms current value is 3.7A.

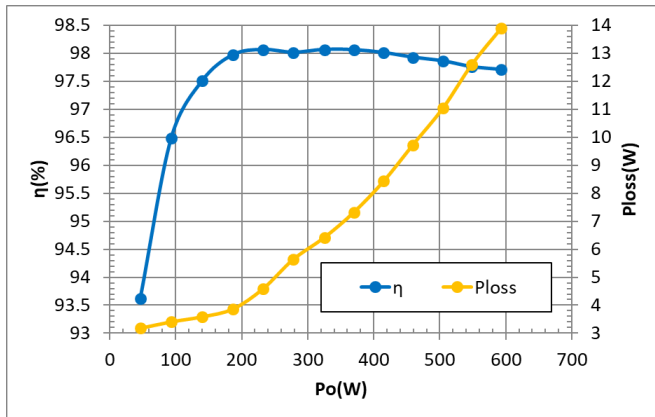


Figure 11. Measured efficiency curve

In Figure 13, the burst mode at light load is achieved. The switching event is enabled every 120ms to conserve power.

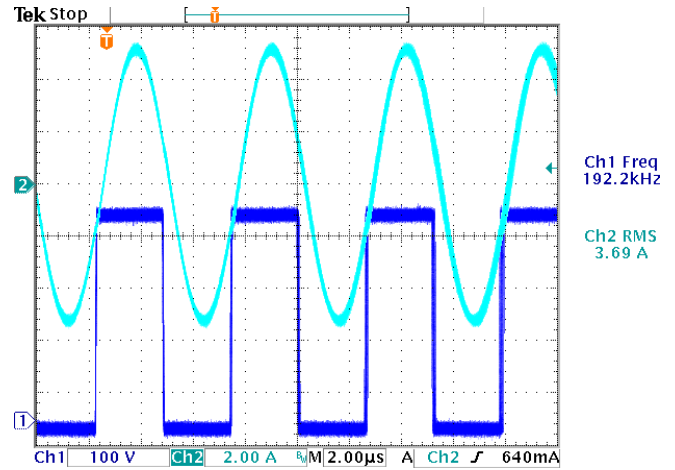
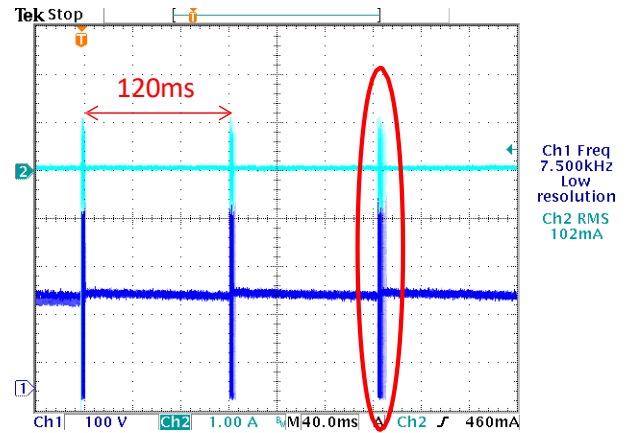
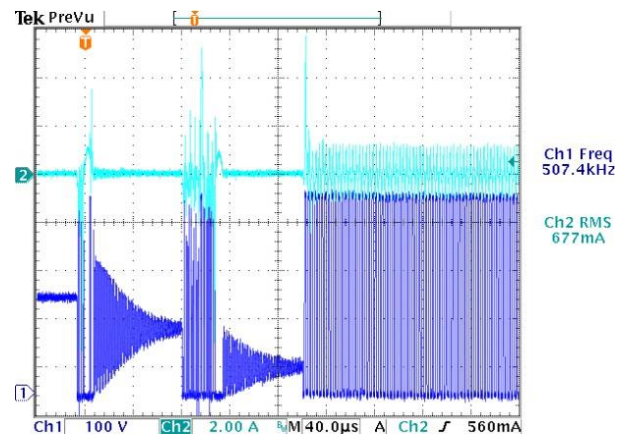


Figure 12. Voltage and current waveform at 600W load



(a)



(b)

Figure 13. Burst mode operation at 0W load: (a) the switching event every 120ms, (b) zoom-in waveform

Reference

[1] Mindy Weisberger, "California Logged Its Hottest Month Ever, and Things are Only Going to Get Worse," Live Science, August 16, 2018, <https://www.livescience.com/63358-noaa-climate-report-and-predictions.html>.

[2] Maria Avgerinou, Paolo Bertoldi, and Luca Castellazzi, "Trends in Data Centre Energy Consumption Under the European Code of Conduct for Data Centre Energy Efficiency," *Energies* 2017, 10(10), 1470; <https://doi.org/10.3390/en10101470>.

[3] G. Spiazzi and S. Buso, "Effect of a split transformer leakage inductance in the LLC converter with integrated magnetics," 2013 Brazilian Power Electronics Conference, Gramado, 2013, pp. 135-140.

[4] Datasheet of TPH3206PS, on-line: <https://www.transphormusa.com/en/document/650v-cascode-gan-fet-tph3206psb/>

[5] Datasheet of TPH3208PS, online: <https://www.transphormusa.com/en/document/650v-cascode-gan-fet-tph3208ps/>

[6] Soft Ferrites and Accessories Data Handbook, 2013, online: <https://www.ferroxcube.com>

[7] Datasheet of NCP1397A/B, online: <http://www.onsemi.com>

[8] Datasheet of NCP4304A/B, online: <http://www.onsemi.com>